



UNIVERSITI PUTRA MALAYSIA

**COLOSSAL MAGNETORESISTANCE
OF $\text{La}_{0.67}\text{Ca}_{0.33}\text{Mn}_{1-x}\text{AxO}_3$ [A = V, Dy AND Zr] PEROVSKITE**

KOH SONG FOO

FSAS 2001 20

**COLOSSAL MAGNETORESISTANCE
OF $\text{La}_{0.67}\text{Ca}_{0.33}\text{Mn}_{1-x}\text{A}_x\text{O}_3$ [A=V, Dy AND Zr] PEROVSKITE**

**By
KOH SONG FOO**

**Thesis Submitted in Fulfilment of the Requirements for the degree of
Master of Science in the Faculty of Science and Environmental Studies
Universiti Putra Malaysia**

April 2001



DEDICATIONS

To Prof. Dr. Halim,
for his patience and guidance....

To my dear family,
Grandma (Tan Kua)
Mother (Tey Hong Eng @ Tey Kim Hong)
Late father (Koh Eng Chuan)
Brothers (Shuang Long and Shuang Par)
Sisters (Sok Hui, Sok Ching, Sok Theng and Sock San)
for their love and concern....

To my dear,
Girl friend (Su Cheng)
for her love, support and understanding....

Fellow friends, ex-coursemates
and University Putra Malaysia as a whole !

Abstract of thesis presented to the Senate of Universiti Putra Malaysia in
fulfilment of the requirements for the degree of Master of Science

**COLOSSAL MAGNETORESISTANCE OF
LANTHANUM MANGANITE PEROVSKITE**

By

KOH SONG FOO

April 2001

Chairman : Professor Abdul Halim bin Shaari, Ph.D

Faculty : Science and Environmental Studies

The colossal magnetoresistive of $\text{La}_{0.67}\text{Ca}_{0.33}\text{Mn}_{1-x}\text{V}_x\text{O}_3$ (LCMVO), $\text{La}_{0.67}\text{Ca}_{0.33}\text{Mn}_{1-x}\text{Dy}_x\text{O}_3$ (LCMDO) and $\text{La}_{0.67}\text{Ca}_{0.33}\text{Mn}_{1-x}\text{Zr}_x\text{O}_3$ (LCMZO), $x=0.00$ to $x=0.30$, ceramics have been studied. X-ray diffraction (XRD) patterns show single-phase perovskite structure with the presence of some minor impurities for all the samples. The systems exhibit tetragonal and orthorhombic distorted perovskite structures, which resulted from the Jahn Teller distortion. Paramagnetic - Ferromagnetic phase transitions were observed in the χ' -temperature curves for all the samples. The Curie temperature, T_C shifts to lower temperature as vanadium, dysprosium and zirconium doping increases respectively, which indicate the loss of ferromagnetic order. Zirconium doping is observed to decrease the T_C more than the effect of other dopants. For LCMVO system, samples with $x=0.01$, 0.02 , 0.03 and 0.30 show an enhancement of volume susceptibility as the temperature increases from $110\text{ K}-140\text{ K}$, $120\text{ K}-142\text{ K}$, $123\text{ K}-140\text{ K}$ and $77\text{ K}-94\text{ K}$ respectively. These enhancements are due to the formation of magnetic clusters

in the samples. For LCMDO system, all the samples show the typical ferromagnetic-paramagnetic transition and no spin glass behaviour was detected. However, in LCMZO system, the samples with $x > 0.05$ show ferromagnetic onset followed by a cusp when cooling from room temperature. The anomalies were due to the formation of spin glass in the sample. The transport properties show the transition of semiconducting to metallic conductivity at T_p . The existence of T_p and T_C was found correlated. This phenomenon of coexistence was due to the double exchange interaction of two electrons in $Mn^{3+}-O^{2-}-Mn^{4+}$ and $Mn^{4+}-O^{2-}-Mn^{3+}$ configuration that brings the system below T_C into a metallic state. The semiconductor model, $\ln(\sigma) \sim (-E_a/kT)$ was used to explain the conduction mechanism of perovskite manganites above T_p . It was concluded that the total conductivity, σ_{tot} , consists of the intrinsic and the extrinsic components. The energy gap found for all the samples was very small and thus exhibits narrow gap semiconductor properties. The measurement of temperature dependence of magnetoresistance has been carried out for each sample. Colossal magnetoresistance value appears at low temperature and the large magnetoresistive effect was observed at temperature approaching T_p . The highest CMR value observed is in LCMZO system for sample with $x=0.14$. The value is 72.2 % at 80 K. However, in LCMVO and LCMDO systems, the observed maximum CMR values are respectively 58.0 % at 170 K for sample with $x=0.20$ and 68.8 % at 126 K for sample with $x=0.20$. For LCMVO system, the increase in CMR value at low temperature may be due to the formation of magnetic clusters.

Abstrak tesis yang dikemukakan kepada Senat Universiti Putra Malaysia sebagai memenuhi keperluan untuk ijazah Master Sains

**MAGNETORINTANGAN RAKSAKSA BAGI
SERAMIK LANTHANUM MANGANITE**

Oleh

KOH SONG FOO

April 2001

Pengerusi : Profesor Abdul Halim Shaari, Ph.D

Fakulti : Sains dan Pengajian Alam Sekitar

Sifat magnetorintangan raksaksa $\text{La}_{0.67}\text{Ca}_{0.33}\text{Mn}_{1-x}\text{V}_x\text{O}_3$ (LCMVO), $\text{La}_{0.67}\text{Ca}_{0.33}\text{Mn}_{1-x}\text{Dy}_x\text{O}_3$ (LCMDO) dan $\text{La}_{0.67}\text{Ca}_{0.33}\text{Mn}_{1-x}\text{Zr}_x\text{O}_3$ (LCMZO), $x=0.00$ hingga $x=0.30$, telah dikaji. Corak belauan sinar-x (XRD) menunjukkan kewujudan satu fasa dengan sedikit bendasing untuk semua sampel. Semua sampel menunjukkan bentuk tetragonal dan ortorombik, akibat daripada herotan Jahn Teller. Peralihan fasa paramagnet-ferromagnet ada dicera pada lengkung χ' -suhu untuk semua sampel. Suhu Curie, T_C masing-masing beralih ke suhu lebih rendah apabila pendopan dengan vanadium, dysprosium dan zirkonium meningkat, menunjukkan kehilangan fasa ferromagnet. Pendopan dengan zirkonium menunjukkan penurunan suhu T_C lebih daripada kesan pendopan lain. Untuk LCMVO sistem, sampel dengan $x=0.01$, 0.02 , 0.03 and 0.30 masing-masing menunjukkan perangsangan pada ketelapan isipadu apabila suhu meningkat daripada 110 K - 140 K , 120 K - 142 K , 123 K - 140 K dan 77 K - 94 K . Rangsangan ini adalah disebabkan oleh pembentukan kelompok magnet di dalam sampel

tersebut. Untuk sistem LCMDO, semua sampel menunjukkan peralihan ferromagnet-paramagnet tipikal dan tiada sifat kaca spin dikesan. Bagaimanapun, dalam sistem LCMZO, sampel dengan $x > 0.05$ menunjukkan permulaan ferromagnet diikuti oleh pembentukan juring semasa penyejukan daripada suhu bilik. Sifat luar biasa ini adalah disebabkan oleh pembentukan kaca spin di dalam sampel. Ciri sifat angkutan menunjukkan perubahan daripada sifat kebolehaliran separa kepada sifat kebolehaliran logam pada T_P . Kewujudan T_P dan T_C didapati saling berkait. Fenomena ini disebabkan oleh interaksi tukarganti ganda dua oleh dua elektron pada konfigurasi $Mn^{3+}-O^{2-}-Mn^{4+}$ dan $Mn^{4+}-O^{2-}-Mn^{3+}$ yang membawa sistem pada paras di bawah T_C ke keadaan pengalir. Untuk sifat angkutan, model semikonduktor $\ln(\sigma) \sim (-E_a/kT)$ digunakan untuk menjelaskan mekanisme konduksi manganite perovskite pada suhu yang lebih daripada T_P . Secara kesimpulannya, jumlah kebolehaliran, σ_{tot} terdiri daripada komponen intrinsik dan ekstrinsik. Jurang tenaga untuk semua sampel didapati sangat kecil dan mempamerkan sifat jurang sempit kebolehaliran separa. Suhu kebergantungan magnetorintangan telah diuji bagi setiap sampel. Nilai magnetorintangan raksaksa muncul pada suhu rendah dan kesan kemagnetorintangan besar diperhatikan pada suhu dekat dengan T_P . Nilai CMR tertinggi dicerap pada sistem LCMZO, bagi sampel dengan $x=0.14$. Nilainya ialah 72.2 % pada 80 K. Walaupun demikian, bagi sistem LCMVO dan sistem LCMDO, nilai maksimum CMR masing-masing ialah 58.0 % pada 170 K untuk sampel $x=0.20$ dan 68.8 % pada 126 K untuk sampel $x=0.20$. Untuk sistem LCMVO, peningkatan nilai CMR pada suhu rendah barangkali disebabkan oleh pembentukan kelompok magnet.

ACKNOWLEDGEMENTS

Firstly, I would like to express my utmost appreciation to Professor Dr. Abdul Halim Shaari, my project supervisor for his patience, ideas, critics, advice, guidance and discussions. I also express my gratitude to my co-supervisor, Associate Professor Dr. Chow Sai Pew and Associate Professor Dr. Hishamuddin Zainuddin for their comments and suggestions throughout the research work.

I am very grateful for the financial assistance provided through PASCA. I would like to thank my friend, Kak Ana, Dr. Rita and all the lecturers in the Physics Department for their comments and discussions. I am very thankful to Mr. Razak Harun for technical favours and other staffs in the Physics Department for their kind help.

Sincere thanks to Mr. Ho Oi Kuan, Ms. Azilah Bt. Abdul Jalil, Mrs. Aminah and staffs from Electron Microscope Unit, Faculty of Bioscience for rendering help in taking SEM micrographs. I am grateful to Dr. Rahim Sahar and En. Jaafar from UTM, Professor Dr. Hamzah Mohamad from UKM and Ling Tze from UPM for allowing the use of the XRD machine.

I wish to thank Dr. S. B. Mohamed and Dr. Azhan B. Hashim @ Ismail for their assistance in using AC susceptometer, resistivity machine and furnace. I am grateful to my friends K.P. Lim and O.S. Yu for helping me during the MR measurement and fruitful discussion. I would like to thank all my labmates,

Kabashi, Malik, Imad, Iftetan, Huda and Talib for their help and understanding regarding this work.

To my friends who always encourage me, Shou Sing, Eng Loke, Hee Chuah, Evon, Lai Soon, Chung Hau, Ee Phing, Fanny, Lucia, Su Kheng and Ei Bee, thanks to all of you. To Ah Mah, Mr. and Mrs. Haw, your support I will never forget.

To grandma, mom, brothers and sisters, your love and support keep me going. To my late father, who leave me in peace, your love and advice always give me high spirit towards my work. I am grateful to my brothers in law, Teck Chuan and Henry, my future brothers in law, Ah Cai and Mike, my uncles and aunts, especially Uncle Choo, who have been concerning about my study all this while. At last but not least, to my girl friend, Su Cheng for her endless love, continuous support, encouragement and understanding.

I certify that an Examination Committee has met on 30th April 2001 to conduct the final examination of Koh Song Foo on his Master of Science thesis entitled "Colossal Magnetoresistance of $\text{La}_{0.67}\text{Ca}_{0.33}\text{Mn}_{1-x}\text{A}_x\text{O}_3$ [A=V, Dy and Zr] Perovskite" in accordance with Universiti Pertanian Malaysia (Higher Degree) Act 1980 and Universiti Pertanian Malaysia (Higher Degree) Regulations 1981. The Committee recommends that the candidate be awarded the relevant degree. Members of the Examination Committee are as follows:

WAN MOHD DAUD WAN YUSOFF, Ph. D.

Associate Professor
Faculty of Science and Environmental Studies
Universiti Putra Malaysia
(Chairman)

ABDUL HALIM SHAARI, Ph. D.

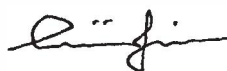
Professor
Faculty of Science and Environmental Studies
Universiti Putra Malaysia
(Member)

CHOW SAI PEW, Ph. D.

Associate Professor
Faculty of Science and Environmental Studies
Universiti Putra Malaysia
(Member)

HISHAMUDDIN ZAINULDIN, Ph. D.

Associate Professor
Faculty of Science and Environmental Studies
Universiti Putra Malaysia
(Member)



AINI IDERIS, Ph. D.

Professor,
Dean of Graduate School,
Universiti Putra Malaysia.

Date: 22 MAY 2001;

This thesis submitted to the Senate of Universiti Putra Malaysia has been accepted as fulfilment of the requirements for the degree of Master of Science.



AINI IDERIS, Ph. D.
Professor,
Dean of Graduate School,
Universiti Putra Malaysia.

Date: 14 JUN 2001

DECLARATION

I hereby declare that the thesis is based on my original work except for quotations and citations which have been duly acknowledged. I also declare that it has not been previously or concurrently submitted for any other degree at UPM or other institutions.



KOH SONG FOO

Date: 29/5/2001

TABLE OF CONTENTS

	Page
DEDICATION.....	ii
ABSTRACT.....	iii
ABSTRAK.....	v
ACKNOWLEDGEMENTS.....	vii
APPROVAL SHEETS.....	ix
DECLARATION FORM	xi
LIST OF TABLES.....	xv
LIST OF FIGURES.....	xvi
LIST OF PLATES.....	xxi
LIST OF ABBREVIATIONS/NOTATIONS/GLOSSARY OF TERMS.....	xxii
CHAPTER	
I INTRODUCTION.....	
What is CMR ?	1
CMR phenomenon	2
Application of CMR Effect.....	3
Objective of the Thesis.....	4
.....	7
II LITERATURE REVIEW.....	
La _{1-x} Ca _x MnO ₃ System (LCMO).....	8
Doping Effect on Mn Site.....	11
La _{0.67} Ca _{0.33} Mn _{1-x} Fe _x O ₃ System (LCMFO).....	11
La _{0.67} Ca _{0.33} Mn _{1-x} Al _x O ₃ System (LCMAO).....	12
La _{0.67} Ca _{0.33} Mn _{1-x} In _x O ₃ System (LCMIO).....	14
La _{0.67} Ca _{0.33} Mn _{1-x} Co _x O ₃ System (LCMCO).....	16
Antiferromagnetic Superexchange.....	17
Jahn-Teller Effect	19
Tolerance Factor	19
Mn Bond Angle and Bond Distance	20
Conduction in Mixed-valence Manganites	21
III THEORY.....	
Introduction To Magnetism	23
Ferromagnetism	23
Antiferromagnetism.....	24
Paramagnetism.....	25
Susceptibility, $\chi = M/H$	27
Curie-Weiss Law	27
Fundamental Information	28
Localized and Itinerant of 3d Electron	29



	Double Exchange Model	29
	Orbital Hybridization and Superexchange	31
	Jahn-Teller Effect	36
	Spin Polaron	37
	Spin Glass	38
	Polaron States in Ionic Crystals	41
IV	SAMPLE PREPARATION AND CHARACTERIZATION.....	42
	Preparation.....	42
	Chemical Powder Weighing.....	42
	Chemicals Mixing.....	44
	Calcination.....	46
	Grinding and Sieving.....	47
	Pressing.....	47
	Final Sintering.....	48
	Sample Characterization	51
	AC Magnetic Susceptibility Measurement.....	51
	Resistivity Measurement.....	53
	Magnetoresistance Measurement.....	55
	X-ray Diffraction Analysis.....	56
	Microstructure Analysis.....	58
V	RESULTS AND DISCUSSIONS.....	60
	LCMVO System	60
	XRD Patterns and Lattice Parameters	60
	Volume Susceptibility and Curie Temperature, T_C	62
	Effect of Field Intensity	66
	Resistivity, ρ and Phase Transition Temperature, T_P ...	69
	Magnetic and Electrical Phase Diagram	71
	Activation Energy, E_a and Total Conduction, σ_{tot}	72
	Microstructure Properties	75
	Magnetoresistance.....	79
	LCMDO system	88
	XRD Patterns and Lattice Parameters	88
	Volume Susceptibility and Curie Temperature, T_C	90
	Effect of Field Intensity	92
	Resistivity, ρ and Phase Transition Temperature, T_P ...	95
	Magnetic and Electrical Phase Diagram	97
	Activation Energy, E_a and Total Conduction, σ_{tot}	99
	Microstructure Properties.....	101
	Magnetoresistance	105
	LCMZO system	111
	XRD Patterns and Lattice Parameters	111
	Volume Susceptibility and Curie Temperature, T_C	113

Effect of Field Intensity.....	116
Resistivity, ρ and Phase Transition Temperature, T_p	120
Magnetic and Electrical Phase Diagram	123
Activation Energy, E_a and Total Conduction, σ_{tot}	124
Microstructure Properties	128
Magnetoresistance	132
Comparison among the Three Systems.....	139
Curie Temperature, T_C and	
Phase Transition Temperature, T_p	139
Activation Energy, E_a	142
Magnetoresistance	144
VI CONCLUSIONS AND SUGGESTIONS	146
Conclusions	146
Suggestions	149
REFERENCES.....	150
APPENDICES.....	155
A Uncertainties of the Equipments.....	156
B Field dependence of the undoped sample of LCMO and doped LCMVO system.....	157
C Field dependence of the doped LCMDO system	163
D Field dependence of the doped LCMZO system	168
E Colossal magnetoresistance as a function of applied magnetic field at different temperature for LCMVO system.....	173
F Colossal magnetoresistance as a function of applied magnetic field at different temperature for LCMVO system.....	179
G Colossal magnetoresistance as a function of applied magnetic field at different temperature for LCMVO system.....	184
VITA.....	189

LIST OF TABLES

Table	Page
2.1 The structure, lattice parameters and transition temperatures of different element doped at Mn site for LCMO ceramics.....	18
4.1 Demagnetization factors, D (SI) for cylinders as a function of the ratio of length to diameter, l/d	51
5.1 Lattice parameters, a , b , c and unit-cell volume of LCMVO system....	62
5.2 Lattice parameters, a , b , c and unit-cell volume of LCMDO system....	88
5.3 Lattice parameters, a , b , c and unit-cell volume of LCMZO system.....	113



LIST OF FIGURES

Figures	Page
1.1 Temperature dependence of resistivity.....	6
1.2 Schematic structure of an ideal perovskite structure.....	6
2.1 The phase diagram of $\text{La}_{1-x}\text{Ca}_x\text{MnO}_3$ system.....	10
3.1 Antiferromagnetic behavior of the sample.....	25
3.2 The atomic spin moment of (a) ferromagnetic, (b) antiferromagnetic and (c) paramagnetic materials.....	26
3.3 Curie-Weiss law shows the presence of paramagnetic phase.....	28
3.4 Schematic illustration of double exchange model.....	31
3.5 (a) Boundary surfaces for angular probability function of $1s$ and $2p$ orbitals (b) Boundary surfaces for angular parts of $3d$ wave functions.....	33
3.6 Schematic illustration of superexchange coupling by σ - transfer and π - transfer.....	35
3.7 Electronic structure of (a) Mn^{3+} in octahedral coordination before and after JT distortion. (b) Mn^{4+} in octahedral coordination.....	37
3.8 Magnetization versus temperature for ZFC and FC.....	40
3.9 Temperature dependence of ac susceptibility (a) in different fields at 100 Hz and (b) in a field of 1 Oe with different frequencies.....	40
4.1 Sample preparation via solid-state reaction.....	43
4.2 Temperature setting for calcination stage.....	49
4.3 Temperature setting for final sintering stage.....	50
4.4 Cylindrical shape of sample.....	53
4.5 Schematic diagram of resistivity measurement.....	54

4.6	Schematic diagram of magnetoresistance measurement.....	55
4.7	Schematic illustration of fundamental process in XRD measurement...	57
5.1	XRD spectrum for all the samples of LCMVO system.....	61
5.2	Thermal dependence of volume susceptibility of LCMVO system at $H=0.1$ Oe.....	63
5.3	Inverse volume susceptibility against temperature of LCMVO system.....	65
5.4	T_C and Θ as a function of vanadium content of LCMVO system.....	65
5.5	Volume susceptibility as a function of vanadium content at 100 K.....	66
5.6	Volume susceptibility as a function of vanadium content at 150 K.....	67
5.7	Abnormal peak of LCMVO system for samples with (a) $x=0.14$ and (b) $x=0.16$	69
5.8	Temperature dependence of resistivity of LCMVO system.....	71
5.9	T_C and T_P as a function of vanadium content of LCMVO system.....	72
5.10	$\ln(\sigma)$ as a function of $1/T$ of LCMVO system.....	74
5.11	Variation of activation energy against vanadium concentration of LCMVO system.....	74
5.12	Sample density of LCMVO system.	75
5.13	SEM image of the fracture surface of LCMVO system.....	78
5.14	CMR curve of LCMVO system as a function of applied magnetic field at 100 K.....	79
5.15	CMR curve of LCMVO system as a function of applied magnetic field at 150 K.....	80
5.16	CMR curve of LCMVO system as a function of applied magnetic field at 170 K.....	81
5.17	CMR curve of LCMVO system as a function of applied magnetic field at 200 K.....	82
5.18	CMR curve of LCMVO system as a function of applied magnetic field at 250 K.....	83

5.19	CMR curve of sample (a) $\text{La}_{0.67}\text{Ca}_{0.33}\text{Mn}_{0.99}\text{V}_{0.01}\text{O}_3$ (b) $\text{La}_{0.67}\text{Ca}_{0.33}\text{Mn}_{0.98}\text{V}_{0.02}\text{O}_3$ (c) $\text{La}_{0.67}\text{Ca}_{0.33}\text{Mn}_{0.97}\text{V}_{0.03}\text{O}_3$ and (d) $\text{La}_{0.67}\text{Ca}_{0.33}\text{Mn}_{0.70}\text{V}_{0.30}\text{O}_3$	85
5.20	CMR curve of sample $\text{La}_{0.67}\text{Ca}_{0.33}\text{Mn}_{0.92}\text{V}_{0.08}\text{O}_3$	86
5.21	CMR curve of LCMVO system as a function of temperature at 1 Tesla.....	87
5.22	XRD spectrum for the samples of LCMDO system.....	89
5.23	Thermal dependence of volume susceptibility of LCMDO system at $H=0.1$ Oe.....	90
5.24	Inverse volume susceptibility against temperature of LCMDO system.....	91
5.25	T_C and Θ as a function of dysprosium content of LCMDO system.....	92
5.26	Thermal dependence of volume susceptibility of LCMDO system at different field intensity when $x=0.12$	93
5.27	Volume susceptibility as a function of dysprosium content at 40 K.....	94
5.28	Volume susceptibility as a function of dysprosium content at 150 K....	94
5.29	(a) and (b) Temperature dependence of resistivity of LCMDO system..	97
5.30	T_C and T_P as a function of dysprosium content of LCMDO system.....	98
5.31	(a) and (b) $\ln(\sigma)$ as a function of $1/T$ of LCMDO system.....	100
5.32	Variation of activation energy against dysprosium concentration of LCMDO system.....	101
5.33	Sample density of LCMDO system.....	102
5.34	SEM image of the fracture surface of LCMDO system.....	104
5.35	CMR curve of LCMDO system as a function of applied magnetic field at 100 K.....	106
5.36	CMR curve of LCMDO system as a function of applied magnetic field at 150 K.....	106
5.37	CMR curve of LCMDO system as a function of applied magnetic field at 170 K.....	107

5.38	CMR curve of LCMDO system as a function of applied magnetic field at 200 K.....	108
5.39	CMR curve of LCMDO system as a function of applied magnetic field at 250 K.....	109
5.40	CMR curve of LCMDO system as a function of temperature at 1 Tesla.....	110
5.41	XRD spectrum for all the samples of LCMZO system.....	112
5.42	Thermal dependence of volume susceptibility of LCMZO system at $H=0.1$ Oe.....	114
5.43	Inverse volume susceptibility against temperature of LCMZO system.....	115
5.44	T_C and Θ as a function of zirconium content of LCMZO system.....	116
5.45	Thermal dependence of volume susceptibility of LCMZO system at different field intensity when (a) $x=0.08$ (b) $x=0.12$ (c) $x=0.14$ (d) $x=0.16$ (e) $x=0.20$ and (f) $x=0.30$	120
5.46	(a) and (b) Temperature dependence of resistivity of LCMZO system..	122
5.47	T_C , T_P and T_{min} as a function of zirconium content of LCMZO system.....	124
5.48	(a) and (b) $\ln(\sigma)$ as a function of $1/T$ of LCMZO system.....	126
5.49	Variation of activation energy against zirconium concentration of LCMZO system.....	127
5.50	Sample density of LCMZO system.....	128
5.51	SEM image of the fracture surface of LCMZO system.....	131
5.52	CMR curve of LCMZO system as a function of applied magnetic field at 100 K.....	133
5.53	CMR curve of LCMZO system as a function of applied magnetic field at 150 K.....	134
5.54	CMR curve of LCMZO system as a function of applied magnetic field at 170 K.....	135
5.55	CMR curve of LCMZO system as a function of applied magnetic field at 200 K.....	136

5.56	CMR curve of LCMZO system as a function of applied magnetic field at 250 K.....	137
5.57	CMR curve of LCMZO system as a function of temperature at 1 Tesla.....	138
5.58	T_C of LCMVO, LCMDO and LCMZO systems as a function of doping concentration.....	141
5.59	T_P of LCMVO, LCMDO and LCMZO systems as a function of doping concentration.....	141
5.60	E_a - intrinsic of LCMVO, LCMDO and LCMZO system as a function of doping concentration.....	143
5.61	E_a - extrinsic of LCMVO, LCMDO and LCMZO system as a function of doping concentration.....	143
5.62	Maximum CMR and respective temperature observed of LCMVO, LCMDO and LCMZO system as a function of doping concentration.....	145

LIST OF PLATES

Plate	Page
4.1 Alumina pot and alumina balls.....	45
4.2 Three-speed electric miller machine.....	45
4.3 Grinder and sieve.....	47
4.4 Hydraulic pressing.....	48
4.5 Tube furnace	50
4.6 AC susceptometer Model 7000.....	53
4.7 Experiment rig for resistance measurement	54
4.8 X-ray diffractometer, Philips (Model PW1830).....	57
4.9 Scanning Electron Microscope (SEM).....	59

LIST OF ABBREVIATIONS/NOTATIONS/GLOSSARY OF TERMS

T	Temperature in Kelvin
T _C	Curie temperature
T _P	Phase transition temperature
T _{SG}	Spin freezing temperature
T _N	Néel temperature
LCMO	La-Ca-Mn-O system
LCMVO	La-Ca-Mn-V-O system
LCMDO	La-Ca-Mn-Dy-O system
LCMZO	La-Ca-Mn-Zr-O system
LCMFO	La-Ca-Mn-Fe-O system
LCMAO	La-Ca-Mn-Al-O system
LCMIO	La-Ca-Mn-In-O system
LCMCO	La-Ca-Mn-Co-O system
CMR	Colossal Magnetoresistance
MI	Metal to insulator
MIT	Metal-insulator transition
MR	Magnetoresistance
GMR	Giant Magnetoresistance
R (H)	Resistance at present of magnetic field
R (0)	Zero field resistance
AFI	Antiferromagnetic insulator
FMM	Ferromagnetic metal

FMI	Ferromagnetic insulator
PMI	Paramagnetic insulator
MRRAM	Magnetoresistive random access memory
R	Trivalent
A	Divalent
$\langle r_A \rangle$	Average ionic radius
t	Tolerance factor
$d_{\text{La-O}}$	La-O bond distances
$d_{\text{Mn-O}}$	Mn-O bond distances
θ	Mn-O-Mn bond angle
θ_{ij}	Angle between spins on neighboring Mn atoms
θ	Bragg angle
τ_h	Electron transfer time
τ_s	Time for a localized Mn spin to relax to a new orientation
D	Demagnetization factor
E_a	Activation energy
DE	Double exchange
JT	Jahn-Teller
ρ	Resistivity
XRD	X-ray diffraction
SEM	Scanning Electron Microscope
d	Sample diameter
H	Applied magnetic field

l	Sample length
M	Magnetization
k_B	Boltzman constant
a, b, c	Lattice parameters
χ	Susceptibility
χ'	Volume susceptibility
μ_{eff}	magnetic moment
AC	Alternating Current
χ_{ac}	AC susceptibility
μ	Magnetic dipole moment
B_{ext}	External magnetic field
C	Curie constant
V	Sample volume
Θ	Paramagnetic Curie point
LSDA	Local spin density approximation
S	Spin electron
l -spin	Localized spin
c -electron	Conduction electron
ZFC	Zero-field cooled
FC	Field-cooled
P	Density
m	Mass
f	Frequency